Comparison of various methods for 3-D eddy current analysis

Takayoshi Nakata
Okayama University

N. Takahashi
Okayama University

K. Fujiwara
Okayama University

Kazuhiro Muramatsu
Okayama University

Z. G. Cheng
Okayama University

COMPARISON OF VARIOUS METHODS FOR 3-D EDDY CURRENT ANALYSIS

T. Nakata, N. Takahashi, K. Fujiwara, K. Muramatsu and Z.G. Cheng*

Dept. of Electrical Engineering, Okayama University,
Okayama 700, Japan
*Baoding Transformer Research Institute,
China

ABSTRACT

Computer codes of the $A-\phi$, $A-\phi-\Omega$, $A^*-\Omega$, $\mathbb{T}-\Omega$ and $\mathbb{E}-\Omega$ methods have been developed, and the accuracy, the computer storage and the CPU time are compared with each other for linear eddy current models. It is shown that the $A-\phi-\Omega$ and $\mathbb{T}-\Omega$ methods are preferable from the viewpoint of the accuracy. The $A^*-\Omega$ and $\mathbb{E}-\Omega$ methods are preferable from the viewpoints of the computer storage and the CPU time.

1. INTRODUCTION

Although various methods, such as the $A-\phi$ [1], $A-\phi-\Omega$ [2], $A^*-\Omega$ [3], $\mathbb{T}-\Omega$ [4] and $\mathbb{E}-\Omega$ [5] methods, have been proposed for 3-D eddy current analysis, the advantages and disadvantages of each method are not discussed systematically until now. It is important to know the most preferable (accurate and fast) method in order to solve a given problem.

We have recently finished the codes for those methods, and the accuracy, the computer storage and the CPU time are compared each other using two linear eddy current models, one of which can be solved analytically, and the other has a hole in a conductor. Two methods for modeling holes in conductors are also investigated.

2. GENERAL DESCRIPTION

2.1 Definitions of variables and basic equations

The number of unknown variables and the CPU time are considerably increased in 3-D eddy current analysis using the $A-\phi$ method, because the magnetic vector potential A with three components is defined in the whole region as shown in Table 1.

In order to reduce the computer storage and the CPU time, various other methods shown in Table 1 are proposed. A^*, $\mathbb{T}$, $\mathbb{E}$, ϕ and Ω are the modified magnetic vector potential, the current vector potential, the electric field strength, the electric scalar potential and the magnetic scalar potential respectively. A^* is defined by the following equation[3]:

$$A^* = A + \int \mathrm{grad}\ \phi\, dt \qquad (1)$$

In those methods except the $A-\phi$ method, the vector quantities A, A^*, $\mathbb{T}$ and $\mathbb{E}$ are defined only in the current carrying region Rj, and the scalar quantity Ω is defined only in the current free region Ro except the $\mathbb{T}-\Omega$ method as shown in Table 1.

Basic equations for those methods are also shown in Table 1. For simplicity, it is assumed that there is no magnetizing current in the analyzed region.

2.2 Modeling of holes

The methods except the $A-\phi$ method shown in Table 1 cannot be applicable to a model with holes, because the magnetic scalar potential Ω cannot be defined in the region where the interlinkage of currents exists[3]. Though two kinds of modeling methods as shown in Fig.1 have been proposed[6] to overcome this difficully, the method shown in Fig.1(a) is not applicable to the $\mathbb{T}-\Omega$ method[7].

The thickness 2D of the thin sheet in Fig.1(a) and the conductivity σ_a of the hole in Fig.1(b) are determined taking into account the accuracy and the CPU time.

Table 1 Various methods for 3-D eddy current analysis

method	variable	basic equation: current carrying region(Rj)	basic equation: current free region(Ro)
$A-\phi$	Ro, A; A, ϕ in Rj	$\mathrm{rot}(\nu\,\mathrm{rot}\mathbf{A}) = -\sigma\left(\frac{\partial \mathbf{A}}{\partial t} + \mathrm{grad}\phi\right)$	$\mathrm{rot}(\nu\,\mathrm{rot}\mathbf{A}) = 0$
$A-\phi-\Omega$	Ω; A, ϕ	$\mathrm{div}\left\{-\sigma\left(\frac{\partial \mathbf{A}}{\partial t} + \mathrm{grad}\phi\right)\right\} = 0$	$\mathrm{div}(-\mu\,\mathrm{grad}\Omega) = 0$
$A^*-\Omega$	Ω; A^*	$\mathrm{rot}(\nu\,\mathrm{rot}\mathbf{A}^*) = -\sigma\frac{\partial \mathbf{A}^*}{\partial t}$	$\mathrm{div}(-\mu\,\mathrm{grad}\Omega) = 0$
$T-\Omega$	Ω; T, Ω	$\mathrm{rot}(\frac{1}{\sigma}\mathrm{rot}\mathbf{T}) = -\frac{\partial}{\partial t}\{\mu(\mathbf{T}-\mathrm{grad}\Omega)\}$ $\mathrm{div}\{\mu(\mathbf{T}-\mathrm{grad}\Omega)\} = 0$	$\mathrm{div}(-\mu\,\mathrm{grad}\Omega) = 0$
$E-\Omega$	Ω; E	$\mathrm{rot}(\nu\,\mathrm{rot}\mathbf{E}) = -\sigma\frac{\partial \mathbf{E}}{\partial t}$	$\mathrm{div}(-\mu\,\mathrm{grad}\Omega) = 0$

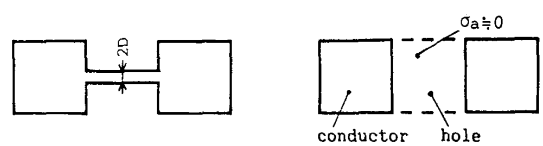

(a) thin conducting sheet (b) conductor with very low conductivity

Fig.1 Modeling methods of holes.

3. COMPARISONS AND DISCUSSIONS

3.1 Description of models

The characteristics of the proposed analyzing method and the validity of the developed software are examined by the following methods:

(1) comparison with the results obtained analytically,
(2) comparison with the experimental results,
(3) comparison with the results obtained by other methods,

0018-9464/88/1100-3159$01.00©1988 IEEE

(4) comparison with the results obtained by other groups.

Two linear eddy current models shown in Figs.2 and 3 are examined to determine the most preferable method for those models. The thin square model shown in Fig.2 is chosen in order to compare the accuracy with the analytical solution[8]. The brick with a hole shown in Fig.3 is chosen as a special eddy current model, in order to clarify the advantages and disadvantages of each analyzing method shown in Table 1.

The conductivity of the thin plate shown in Fig.2 is 1.0×10^7(S/m). The applied magnetic field in the z-direction is uniform in space and changes with time as follows:

$$Bz = \begin{cases} 0 & t < 0 \\ 1000\cdot t \ (T) & t \geq 0 \end{cases} \tag{2}$$

The number ne of tetrahedral elements is equal to 8586.

The conductivity σ_c of the brick shown in Fig.3 is 0.25×10^8(S/m). The conductivity σ_a of air inside the hole corresponding to Fig.1(b) is chosen as 1(S/m)[4] for the T-Ω method, and zero for the other methods. The conductivity of the thin sheet shown in Fig.1(a) is the same as σ_c of the brick. The applied magnetic field in the z-direction is uniform in space and decays exponentially with time as follows:

$$Bz = 0.1\, e^{-t/0.0119} \tag{3}$$

The number ne of elements is equal to 10098.

1/8 of the whole region is analyzed in each model. The time interval of the step-by-step method[9] for solving the transient phenomena is 1(msec).

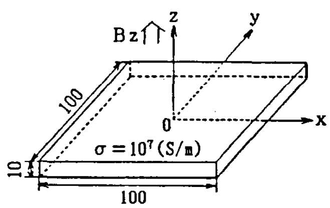

Fig.2 Square plate.

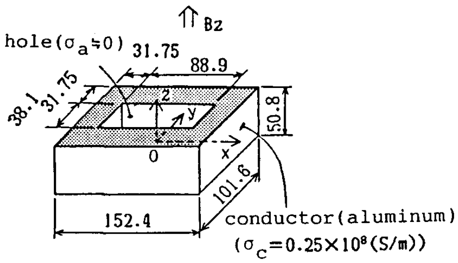

Fig.3 Brick with a hole.

3.2 Comparisons of two methods for modeling holes

The suitable thickness D of the thin sheet shown in Fig.4 is investigated, and both the methods shown in Figs.1(a) and (b) are compared each other in terms of the accuracy and the CPU time.

Figure 5 shows the effect of D on |Iea|/|Ieb| in the case of the A^*-Ω (E-Ω) method. Iea and Ieb are the eddy currents at 10(msec) flowing through the cross sections of the thin sheet (hatched) and the conductor (dotted) respectively as shown in Fig.4. L is the half thickness of the conductor. Figure 5 denotes that D/L should be less than 0.03 under the condition that the eddy current in the hole is within 1(%) of that in the conductor. Table 2 shows the number ni of iterations of

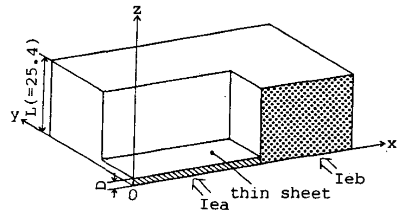

Fig.4 Thin sheet.

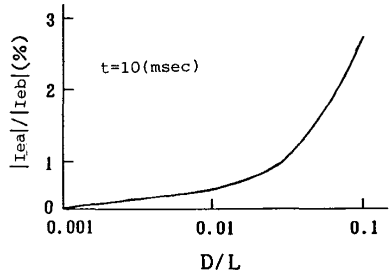

Fig.5 Effect of D/L on |Iea| / |Ieb| (A^*−Ω(E−Ω) method).

Table 2 Comparison of two kinds of methods for modeling hole (A^*−Ω(E−Ω) method)

method	thin sheet (Fig.1(a), Fig.4)			low conductivity
	D/L=1/10	1/100	1/1000	(Fig.1(b))
number ni of iterations of ICCG method	66	175	746	71
CPU time (sec)	107	221	814	116

Computer : SX-1E (NEC supercomputer)

the ICCG method and the CPU time for various D/L. The computer codes are not vectorized. The number ni is rapidly increased when D/L is decreased. This is because the coefficient matrix becomes ill-conditioned when D/L is small.

The flux and eddy current distributions calculated by both methods shown in Fig.1 are almost the same. The number ni and the CPU time of the method shown in Fig.1(b) are also denoted in Table 2.

Almost the same results can be obtained for the A-ϕ-Ω method.

3.3 Accuracy

The accuracy of each method shown in Table 1 is compared with analytical solutions using the thin plate shown in Fig.2. Figure 6 shows the time variations of the x-component, J_{ex} and the absolute value $|J_e|$ of the eddy current density. The analytical solution at the steady state is also shown in Fig.6. The accuracy of each method can be checked by comparing results obtained near steady state limit (t=15(msec)). As the results of T-Ω (---) and that of A-ϕ-Ω (——) are almost the same, they are overlaped in Fig.6. The result of the A^*-Ω(E-Ω) method is a little different from the analytical one. Figure 6 suggests that the A-ϕ-Ω and T-Ω methods are preferable from the viewpoint of the accuracy.

The accuracy is also compared for each method for the conductor with a hole shown in Fig.3. Figure 7 shows the comparison of the total circulating current (eddy current) calculated by each method. In this situation, the differences among the $A-\phi$, $A-\phi-\Omega$, $A^*-\Omega(E-\Omega)$ and $T-\Omega$ methods are larger than those for the case of Fig.6.

3.4 Computer storage and CPU time

Table 3 shows the comparison of the computer storage and the CPU time for the model shown in Fig.2. In this case, the eddy current is analyzed taking into account three components of vector quantities. The CPU time of the $A^*-\Omega(E-\Omega)$ and $T-\Omega$ methods can be considerably reduced to less than 1/10 compared with that of the $A-\phi$ method.

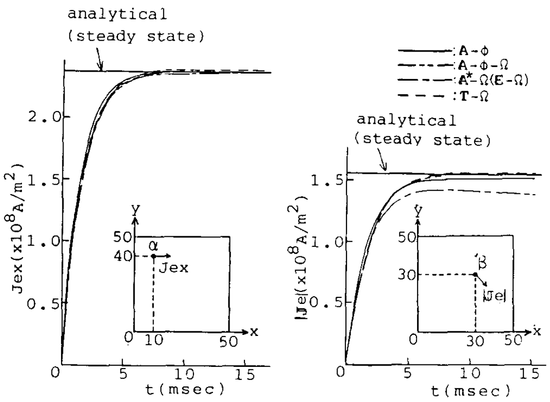

(a) point α (b) point β

Fig.6 Time variations of eddy current density (z=1.67(mm)).

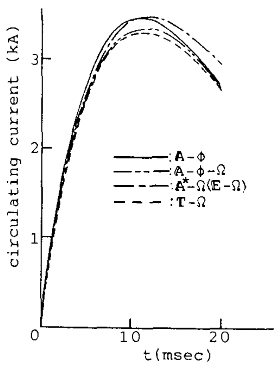

Fig.7 Total circulating currents.

Table 3 Comparison of computer storage and CPU time (Fig.2)

method	number of unknown variables	computer storage (MB)	CPU time (sec)
$A-\phi$	4712	5.5	751
$A-\phi-\Omega$	2788	3.9	253
$A^*-\Omega(E-\Omega)$	2208	3.2	68
$T-\Omega$	2208	3.3	63

computer : SX-1E (NEC supercomputer)

Table 4 shows the comparison for the model with a hole shown in Fig.3. It suggests that the CPU time of the $T-\Omega$ method is not decreased much due to the ill-condition of the coefficient matrix when the hole is modeled by the conductor with very low conductivity.

Table 4 Comparison of computer storage and CPU time (Fig.3)

method	number of unknown variables	computer storage (MB)	CPU time (sec)
$A-\phi$	5512	6.5	1912
$A-\phi-\Omega$	3592	4.9	498
$A^*-\Omega(E-\Omega)$	2824	3.9	116
$T-\Omega$	3064	4.2	851

Computer : SX-1E (NEC supercomputer)

4. CONCLUSIONS

The accuracy, the computer storage and the CPU time of various methods are compared.

The obtained results can be summarized as follows:

(1) From the viewpoint of the accuracy, the $A-\phi-\Omega$ and $T-\Omega$ methods are preferable.

(2) From the viewpoints of the computer storage and the CPU time, the $A^*-\Omega$ and $E-\Omega$ methods are preferable.

More systematic comparisons of various methods will be reported later.

ACKNOWLEDGEMENT

This work was partly supported by the Grant-in-Aid for Fusion Research from the Ministry of Education, Science and Culture in Japan (No.62050013).

REFERENCES

[1] M.V.K.Chari, J.D'Angelo, M.A.Palmo & D.K.Sharma : "Application of Three-Dimensional Electromagnetic Analysis Methods to Electrical Machinery and Devices", IEEE Trans. Energy Conversion, EC-1, 2, 151 (1986).

[2] A.Kameari : "Three Dimensional Current Calculation Using Finite Element Method with A-V in Conductor and Ω in Vacuum", IEEE Trans. Magnetics, MAG-24, 1 (1988).

[3] C.R.I.Emson & J.Simkin : "An Optimal Method for 3-D Eddy Currents", IEEE Trans. Magnetics, MAG-19, 6, 2450 (1983).

[4] T.Nakata, N.Takahashi, K.Fujiwara & Y.Okada : "Improvements of T-Ω Method for 3-D Eddy Current Analysis", IEEE Trans. Magnetics, MAG-24, 1 (1988).

[5] I.D.Mayergoyz : "3-D Eddy Current Problems and the Boundary Integral Equation Method", Computational Electromagnetics, (book), Elsevier Science Publishers B.V.(North-Holland), 163 (1984).

[6] D.Rodger & J.F.Eastham : "Multiply Connected Regions in the A-Ψ Three-Dimensional Eddy-Current Formulation", Proc. IEE, 134, A, 1, 58 (1987).

[7] T.W.Preston & A.B.J.Reece : "Finite-Element Solution of 3-Dimensional Eddy Current Problems in Electrical Machines", Proceedings of COMPUMAG Conference, Grenoble, 7.4 (1978).

[8] D.W.Weissenburger & U.R.Christensen : "Transient Eddy Currents on Finite Plane and Toroidal Conducting Surfaces", Plasma Physics Laboratory, PPPL-1517 (1979).

[9] T.Nakata & Y.Kawase : "Numerical Analysis of Non-Linear Transient Magnetic Field by Using the Finite Element Method", Electrical Engineering in Japan, 104-B, 6, 81 (1984).